Jurnal Kejuruteraan 36(5) 2024: 1955–1963
https://doi.org/10.17576/jkukm-2024-36(5)-15

File Encryption by Iris Recognition System

Musab A. M. Ali[b*], Nooritawati Md Tahir[d] & Israa Al-Rawe[c]

[a]*College Of Computing And Information Sciences,*
University Of Technology And Applied Sciences, Sultanate Of Oman

[b]*Department of Cybersecurity,*
International Information Technology University, Almaty, Kazakhstan.

[c]*Technical Engineering College,*
Northern Technical University, Mosul, Iraq

[d]*Faculty Of Electrical Engineering,*
Universiti Teknologi Mara (UiTM), Malaysia

**Corresponding author: musab.alrawi@utas.edu.om*

Received 11 February 2024, Received in revised form 13 May 2024
Accepted 11 July 2024, Available online 30 September 2024

ABSTRACT

This paper designs a framework for an iris recognition system to obtain significant information by encryption and decryption using iris recognition system to improve the security level of stored extended data. Iris feature to confirm the character of an individual person to grant access to the information document. The strategy is extracted using 1D filter Log-Gabor which has high decidability and minimum variance between (inter & intra) class. In this paper, the 1D filter Log-Gabor was applied, the results are based on FAR and FRR, as feature selection models with SVM type nonlinear quadratic as classifiers CASIA datasets were used. The iris image captured by a high-resolution webcam is used to enter a record that identifies the eligible individual as the beneficiary. The prepared image is matched with the registered iris in the dataset and only if a match is found, it is included in the file. It adds to the assortment of information by providing evidence of the usefulness of the iris in verifying the person, it shows that the iris is very reliable. Segmentation specific area only clarifies the exhibit of this exploration work novel strategy among iris segmentation procedures, all together in restricting the pupil before limiting the iris.

Keywords: Iris recognition; SVM; 1D filter Log-Gabor; FAR and FRR

INTRODUCTION

The privilege of the iris and the left and right eye are extraordinary. The human iris is constant throughout life. The characteristics of the iris do not change with age but stand out from other biometric characteristics, such as the voice, fingerprints, and face. The higher level of accuracy in biometrics is iris recognition, also appeared more useful differently in terms of an exceptional imprint, face, retina, and voice (Drozdowski et al. 2019). Iris recognition framework combines PC vision, experience, and model recognition. The advancement is a highly secure recognition framework to the person nature of a human being through logical examination of unpredictable boundary within the iris, the boundary is recognizable and is taken by different partition. These boundaries are consistent throughout life because the iris is a guaranteed inner organ. It can give expression as such a living secret that need not be remembered but is largely passed on (Gumaei et al. 2019). The system controls access to resources that require identifiable proof of individuals, to which only approved individuals have access. Presently, most high security level controls are open to iris recognition, for example, cell phones, windows, and structures that incorporate profound identification. numerous applications that utilize iris recognition frameworks, for example, at line crossings, likewise at flight terminals for passenger evaluation for long-time clients (Ahmad et al. 2019). In this work, the framework works by capturing a high-resolution eye by means of a webcam, the highlights of the iris are analysed against a record with the goal that the person's personality permits entry to file. Iris recognition is non-intrusive because a person has no compelling reason to order to use the system. The iris recognition framework will be less costly because the utilization of webcam in any computer, additionally programmed with auto center, and the recognition speed makes the framework simple to utilize, a person is consequently distinguished after moving towards the iris image. When looking at the webcam from a distance of 3-10", The computer webcam captures the entire face and then segments the image to obtain the eye only, which is processed into a 4800-iris code and stored in the database.

Essentially, all biometric frameworks. start with catches an example of the biometric features, at that point extricated and changed it into numerical code over to store into the data set. Unpredictable examples were taken to build the data collection, these examples are stored as an iris code into the data collection to be used for testing and preparing an approved individual. ID confirmation, the iris highlights should be broken down with the data collection when the memory closes on that approved individual (Pernaet al. 2017). Most experiment in biometrics is the iris, the activity of dilator is the extent of light entering the eye through the pupil, notwithstanding that it is also an enhancement of the versatile connective tissue that gives it a tangled, fibrillar model. Recognized biometrics utilized is anatomical, for example, facial look, hand, fingerprints, retinal vein models, and iris plans (Ogbanufe et al. 2018). Biometrics has been around since 1980, but only now has it begun to gain a foothold in the preparation and correspondence industry for client applications (Sujatha et al. 2018). Although easy to recover and replace, computerized data is more helpless against programmers and leeches. The utilization of physical records and cabinets to keep data has been supplanted by PCs; this enables associations and individuals to store such significant resources in computerized forms (Murdock et al. 2017). To improve security by restricting access just to those who have authorization. in conventional strategies and additionally, biometric qualities other than iris, give such control; yet despite everything, they have a couple of limitations in confirming the recognizable proof. In this paper, created and improved the security of data on file by controlling access thoughts recognising system prerequisites that are identified with iris recognition and testing the neural system.

Extensive testing is to find out which methods give the ideal execution of framework activity, the goal of minimizing FRR stands for False Reject Rates, FAR stands for False Accept Rates but increasing RR stands for Recognition Rate, also increasing system speed to develop a profoundly usable to secure the file information by design framework for biometric iris recognition, in addition to decreasing degrees of freedom (DOC) in iris format representation. Iris recognition fruitful execution of pupil recognition task the masking technique applied. Hough Transform used to find the iris boundary, the task of selecting the correct circles from all the collector maxima completed without any problems. Overall, the masking technique has facilitated the resulting cycles of the framework. The personal identification system for locking/unlocking, as shown in Figure 1, is composed of the following steps:

1. Right click on the file, then the iris recognition system will be activated.
2. Take a picture of the face and do the segmentation for the eye and from the webcam height accuracy.
3. Convert the iris into a code and save it in the database.
4. The code for iris will be used for back Back-probagation.
5. New users are stored in the database, otherwise the pattern of the existing user is compared with the data set.
6. Detection of signal end or return.

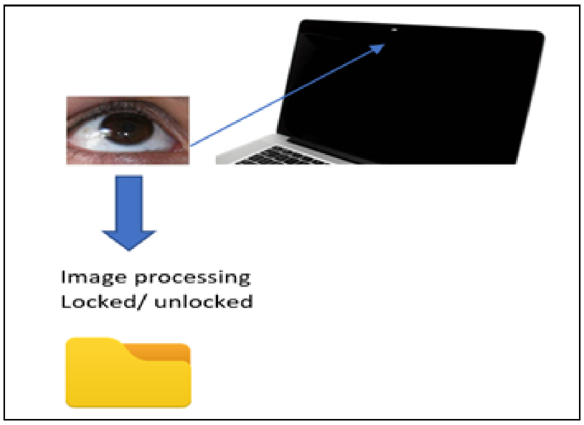

FIGURE 1. Locked / Unlocked FILE

RELATED STUDIES

The iris is a coloured round muscle, which is wonderful and gives a shade to the eye. The size of the iris is controlled by the round muscle with the goal that quite a bit of light can get into the eye, contingent upon the illumination conditions (Nguyen et al. 2017). The iris, as shown in Figure 1, includes lines, spots, rings, cracks, pits, graves, spots, stripes, constriction folds, crowns, and serpentine vessels (Adamović et al. 2020). Researchers have distinguished 250 Parameters from the iris of any individual, as opposed to about 40 for fingerprints. established by a person's life, however, another biometric can be altered by modification or damage, such as the voice or a face, a unique mark and hand pattern. Considering the fact that iris ID is more accurate than the other accessible high-method discrimination detection systems that examine voices, faces and fingerprints (Trokielewicz et al. 2020).

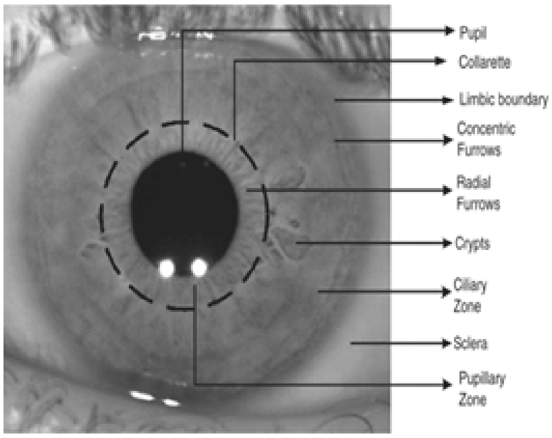

FIGURE 2. Iris Features

From Figure 2, the most independent biometric component in the human body is the iris. No two irises resemble each other, even in twins (Barpanda et al. 2019). The probability that two irises are never the same is rated as 1 out of 1072. In this way, iris recognition is factually more accurate than DNA testing (Gruenenberg et al. 2020). Considering these iris designs, there's a way to deal with a definite clear recognition of people when the iris should be possible within the measuring device, and basically when to look in huge datasets with the fewest false matches despite a colossal number of possible results. Albeit small, that is 11mm in size, and the iris has the incredible numerical favorable position that its parameter is huge among different people. The shading of the iris is determined by the thickness of the melanin pigment in the anterior layer and the stroma, the blue iris resulting from the nonappearance of coloured long-wavelength light, while the shorter wavelengths are scattered by the stroma. In any case, the iris design is exceptionally differentiated, as the recognizable detection technique proves more challenging. The quantity of evaluations between the biometric test and formats decides on an essential separation between the two techniques for performing biometric confirmation: Confirmation and identification. In confirmation mode, also called productive confirmation, the system checks the validity of whether a declared person can access or not. For this reason, the biometric test, for example, the personality of the subject person should be passed to the confirmation computation. Also, the evaluation is done between the biometric design and the model. The similarity is sufficiently high, and the guaranteed person affiliation is confirmed, which means that both biometric features have been separated from a similar individual. In identification mode, the characteristics of a person are compared with those of numerous individuals to show that a person is not expected that the precision and straightforwardness of the application of the iris recognition system will attract attention, around the globe as open well-being, escape, instruction, and social security (soliman et al. 2020). Among the models are those utilized in expansive and little-area remedy systems in the United States (Chen et al. 2020),

CASIA-A DATABASE

The CASIA dataset stood from the Chinese Academy of Sciences Institute of Automation used in this paper. The dataset contains 2,700 iris images of 250 in different subjects, JPEG design with (320x280) targets. The iris images were acquired under exceptionally difficult acquisition conditions and have close and homogeneous features. The confounding factors were from eyelids and eyelash obstructions. In addition, the iris images were subjected to post-processing in which the pupil regions were filled with dark pixels. Figure 3 shows iris images from the (CASIA 2019).

FIGURE 3. Eye Sample from CASIA

METHODOLOGY

Since 1987, when the primary important philosophy of Flom was introduced, various increases have been proposed (Trokielewicz et al. 2020). The pertinent techniques, the reason for some working frameworks, in the division phase, presented a vital distinction administrator with both inner and outer iris borders. Administrator remains real and was proposed with some little contrast (Hofbauer et al. 2019). The integrodifferential administrators looking over an N3 space that has as its goal the expansion of the condition to establish the iris fringes and iris division (Spettel et al. 2019) through an inclination based on a twofold border outline followed by Round Hough. it is the most widely used system that has been proposed with some minor parameters. Strategy based on limit and capacity amplification, with the end goal of acquiring ring parameters compared with the inner and outer edges of the iris (Rivetti et al. 2020). Technique for iris localization based on the earlier detection of pupil detection. The image is then converted to polar directions and the outer edge of the iris is detected as the largest uniform edge resulting from Sobel sighting. The methodology fails for non-concentric iris and pupil, taps, and exceptionally "dim" iris areas (Wang et al. 2021).

INTEGRO-DIFFERENTIAL OPERATOR

To detect the circumferential iris and the locations of a pupil, in addition to the upper with lower eyelids, the integro-differential operator is used (Sahmoud et al. 2020). The integrodifferential operator is described by.:

$$\max_{(r, x_0, y_0)} \left| G_\sigma(r) * \frac{\partial}{\partial r} \oint_{(r, x_0, y_0)} \frac{I(x, y)}{2\pi r} \, ds \right|$$

Here I (x, y) is the full eye image, to be searched inside the eye use "r" for the radius, the Gaussian filter uses "Gσ (r)", and the contour number uses "s", the full circle by (r, x, y). By different the radius and centre "x and y" of the circular contour, the circle in which the maximum change in pixel values occurs is found. Applied iteratively, gradually reduce the degree of smoothing to achieve precise localization. The eyelids are delineated along these lines, how the shape is adopted changing from round to curved.

NOISE DETECTION

Consider the districts in the iris such as eyelashes or eyelids as noise should be removed using a Hough transform edge detector. A proposed method that uses the directional filter for eyelash and eyelid edge detection. The eye image contains eyelashes, the exploratory design of the directional filter and Figure 4, shows the eyelash on the CASIA dataset.

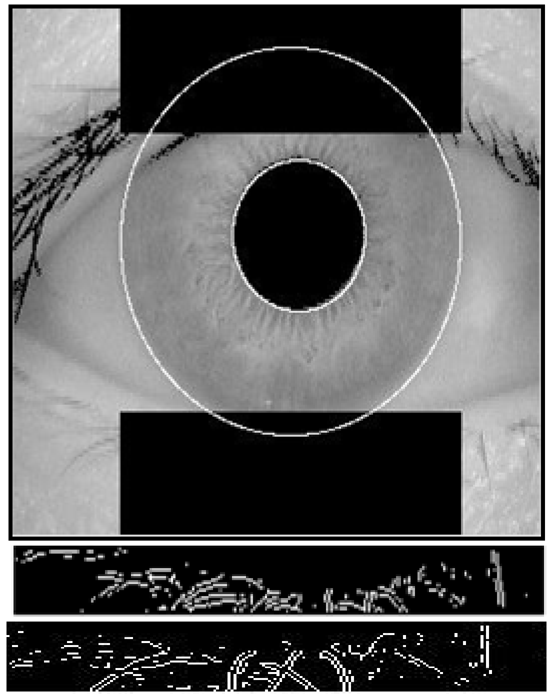

FIGURE 4. Top & Bottom of Eyelash

The directional filter gives a good result and is easier to implement. The exploratory effect of noise reduction with the straight Hough transforms and a threshold as shown in Figure 5.

FIGURE 5. Noise Occlusion Process

Execution time of the aperture constraint since the image in the CASIA dataset has a resolution of (1280 x 960). Therefore, arrange the image target at five in a different code size. The correlation effects of implementation of time based on the eye image target for the image dataset as shown in Table 1.

TABLE 1. Execution time comparison of multi-resolution

Code Size	4800	1920	960	480	240
Iris	0.9	0.89	0.79	0.72	0.7

As demonstrated in Table 1, the execution time also increases as the target increases. The execution time for iris detection was about 0.9 ms at code size (4800) by using the circular Hough transform. After resizing the code size (1920), the execution time reduces to 0.89 ms. And by further limiting the code size (960), the execution time reduces to 0.79 msec. Reshaping the code size (480) reduces the execution time to 0.72 msec. Finally, reshaping the code size (240) reduced the execution time to 0.7 msec. In short, from the image of a full code size of 4,800. Then it is reshaped to two type of code sizes: 1,920 and 960. By reshaping it again, get an iris with a code size of 480 and 240. The code size of 480 is basically the reasonable code size, because below that the image is not recognized, and if it is above 480, the results are just similar regular results obtained from half an eye.

NONLINEAR CLASSIFICATION

Nonlinear classification, usually the resulting computation is particularly similar, separate from replacing each point with an element of a nonlinear piece. Subsequently, this algorithm can be used to set a hyperplane with the most extreme edge in a modified point space. The transformation used nonlinear, and the altered highlight space is in a high degree. Therefore, even if the classifier hyperplane is in the high dimensional feature space, it will generally be nonlinear in the first space as described (Song *et al.* 2019). The piece utilized is a Gaussian function, the comparative highlight space is in this way a Hilbert space of unbounded measurements (Gu *et al.* 2021). Additionally, the greatest edge classifiers are strongly regularized, the outcomes are essentially attainable without being destroyed by the infinite measurements. The following are the used kernels: -

Hyperbolic tangent: k(xi,xj) = tanh (kxi.xj + c), for some (not every) $\kappa > 0$ and $c < 0$

GABOR FILTERS

The bottom of the Gabor filter is more remarkable than an octave every time; the real filter will be a DC part. Regardless, utilizing Gaussian on a logarithmic scale, a zero DC segment is attainable for each data transmission (Barpanda et al. 2019). The recurrence response of a Log-Gabor filter is determined by:

$$G(f) = exp((-(\log (f/f\_0))\hat{}2)/(2(\log (\sigma /f\_0))\hat{}2))$$

Here, the center frequency is represented by (f0) while (σ) indicates the filter bandwidth. The outputs of the Gabor filter are demodulated to obtain the information in a condensed form. The stage data are quantized into the degree of four, for each probable quadrant in the perplexity. When examining the data of the stage and the data of the fullness, the previous gives the main data within an image. To encode the separating data in the aperture, simply the stage is taken, in the meantime, the part of adequacy that addresses the wealth data like enlightenment is discarded. Two bits of information are used to address the four degrees of quantized stage data. Each pixel in the standardized example of an iris corresponds to two bits of information in the format of an iris. A few frameworks utilize polar coordinates for normalization (Selvamuthu et al. 2020), The (r_0, θ_0) specify the filter center frequency. along these lines as polar the filters are determined by:

WAVELET LOG-GABOR FILTRE

Highlight coding is performed by convolving the standardized iris design with the 1D wavelet Log-Gabor. Different 1D characters are isolated from the standardized 2D example and then convolved with a 1D Gabor wavelet. The regions of the standardized 2D example are represented as 1D characters, with each line compared to a round ring on the iris location. Since the greatest self-regulation happens on the precise path and not on the extended path, the one that is comparable to the standardized example pieces is taken. The 2D Gabor filter is executed by convolving the 2D normalized aperture pattern with the 2D Gabor filter. To expect the influence of the perturbation in the filter yield, the highest points of the power at known perturbation regions in the standardized model are set to the ordinary power of the enveloping pixel. The period of the yield from the filters is quantized to four levels (two pieces). The quantized examples are encoded using the dim code. In this way, the number of disconnected pieces is reduced.

Moreover, this turns an increasingly precise recognition into two to some degree skewed two intra-class designs. The path to encoding leads to a reasonably clever layout that contains different bits of data, as a relational concussion veil (Muthukumar et al. 2019). This concussion veil refers to deteriorated zones within the iris design. In districts where adequacy is (zero), the stage data has no significance and, in the commotion, veil these areas are stamped. A complete piece of the format is achieved depending on the magnification of the rakish target times the spiral target. Applying the eye quarter decreases the degree of the eye's shock, then additionally decreases the goof, and increases the accuracy.

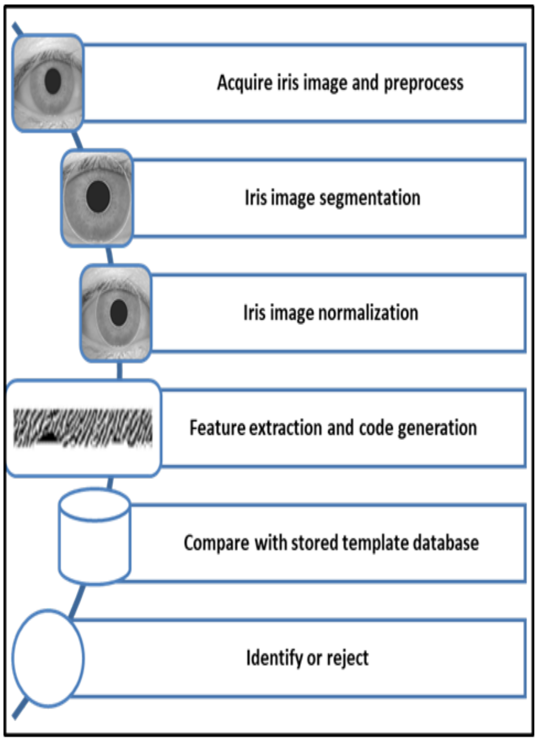

FIGURE 6. Algorithm Person Identification

The system person identification as shown in Figure 6:

1. Capturing the eye image from the webcam.
2. According to the location of the eye, the iris is delineated by the fine boundary between the pupil and the iris.
3. The area of the pupil is obtained, the preference and the left deflection of the iris are separated.
4. The feature of the iris is extracted by set the polar coordinate system.
5. The extracted iris parameter is split into traces as a band.

ACCURACY MEASUREMENT

The performance of a biometric structure is estimated by its accuracy in recognizing authorized individuals and rejecting authorized individuals. An appropriate threshold for the chosen standard is significant. The FAR also (FRR) are typically implemented to quantify the accuracy of all the types of biometric structures. The inability to pick and inability to gain rates are likewise considered in biometrics. Furthermore, the replacement time and effort in a representation of the biometric structure sometimes are likewise evaluated. The quantity of non-authorized is falsely assumed from the structure, Refers False Accept Rate (FAR). FAR percentage of a bogus authorization to be found by the biometric framework.

$$FAR\ (percent) = ((Number\ of\ false\ accept) / (Total\ number\ of\ accepts\ by\ the\ system)) * 100\ percent$$

The amount of data falsely rejected by the frame. It is considered as the percentage of an enrolled client who was denied authorization by the biometric framework.

$$FRR\ (percent) = ((Number\ of\ false\ reject) / (Total\ number\ of\ rejects\ by\ the\ system)) * 100\ percent$$

Recognition Rate (RR) – Refers to the (FAR and FRR) are equal.

$$RR\ (percent) = [100 - (FAR + FRR)]$$

RESULTS

The iris recognition structure has excellent advantages such as change, strength, and security. Consequently, it has a wide range of uses. A different and incredible iris calculation has been carried out dealing with eigen iris, where the centroid of each iris recognition depends on the Euclidean distances. The results were obtained utilizing four iris images for preparation; similarly, it is critical to add another class to re-train the system. The different arrangement images affect both the recognition rate and the speed of CPU. All data were acquired using a webcam. Figure 7 shows the image accuracy and the different trapping speed. As the capture ratio increases, the accuracy also increases.

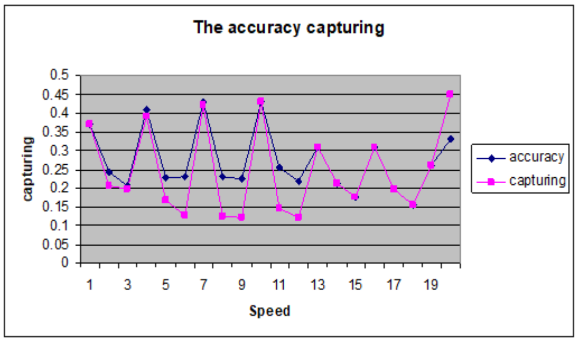

FIGURE 7. Relative (Accuracy & Speed)

The dataset contains iris codes of people who can gain access to a file. MATLAB (R2020b) is used to contrast a person's iris and the dataset. Figure 8 shows the Relative between the dataset sizes and the speed examination.

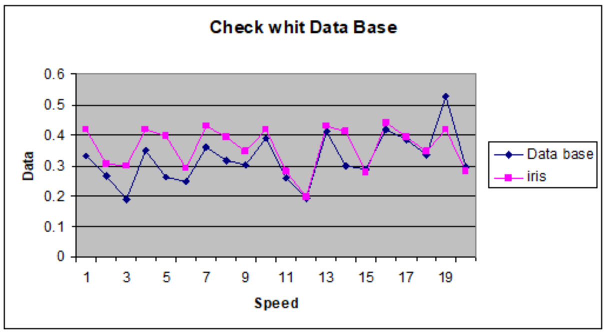

FIGURE 8. Relative research the iris in database

The processor converts the iris to code, as demonstrated in Figure 9. The conversion of each iris into code for storage in the information base is an extraordinarily fundamental advance. This conversion is done after the iris image is captured in a simple manner. It is transformed by removing 160 boundaries from each picture. Cleaning of the images is also done in a similar procedure. shows the diagram of iris processing versus time spent.

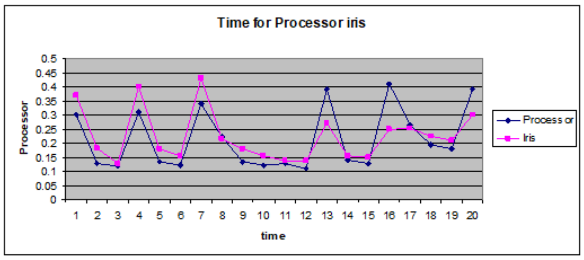

FIGURE 9. Relative (Accuracy and Time)

1D LOG-GABOR FILTER

1D Log-Gabor filter used for the recognition system gives a great result, high decidability with the minimal difference between both variables inter-class and intra-class. Figures 7 show the results decision criterion with FAR and FRR used the 1D Log-Gabor filter, the classifiers used SVM (Nonlinear Quadratic kernel). Most commercial iris recognition frameworks utilize patented computations developed by Daugman, and indeed these computations can produce wonderful recognition rates, decidability, and least changes/differences between (inter- and intra) class variables. In this paper, the values of decidability and least difference generated from encoding formats using a 1D filter Log-Gabor with different radial and precise target dimensions are given in Table 2.

TABLE 2. The Decidability by 1D Log-Gabor Filter with Various Code Sizes

Code size	σ Intra-class	σ Inter-class	μ Intra-class	μ Inter-class	Decidability	Min diff
240	6.9E-03	6.5E-03	0.2145	0.3058	1.1068	0.338
480	4.1E-03	4.0E-03	0.2087	0.3268	1.8274	0.219
960	2.9E-03	1.8E-03	0.2587	0.4075	3.4765	0.179
1920	1.9E-03	8.7E-04	0.2793	0.4345	4.2333	0.149
4800	1.7E-03	3.4E-04	0.2862	0.4692	5.6657	0.121

As shown in Figure 10, the FAR /FRR datasets with SVM (nonlinear), used the 1D Log-Gabor as a function of the decision criterion.

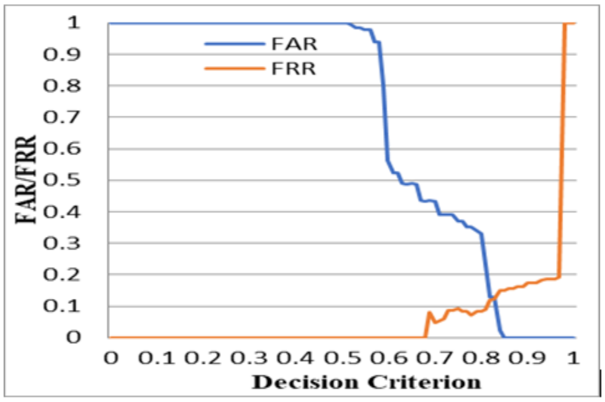

FIGURE 10. FAR & FRR with DC.

As shown in figure 10, the SVM (Nonlinear), is proved that gives excellent results. In Table 3, the results of RR using 1D filter Log-Gabor with the application of SVM (Nonlinear) are given.

TABLE 3. The RR used filter of 1D Log-Gabor.

Decision criterion	SVM (nonlinear)		
	FAR	FRR	RR
0.77	0.2	0.2	99.7

As shown in Table 3, SVM (nonlinear) is the best determination when applied 1D Log-Gabor as it gave 99.7% of detection rate, also minimum FAR and FRR 0.2% as individually and gave the high decision criterion of 0.77. The primary element of this present proposed framework is obviously possible and imperative for a biometric recognition framework.

CONCLUSION

Highly privileged data in files by using biometric specifically iris recognition system. In this work, an iris system was planned that includes an inherent webcam PC and a composite program consisting of the main image, which obtains an enhanced iris pattern image, and a second neural association for recognition using the iris design data. The neural association stage includes two stages: the first preparation stage for discriminating the human iris and the testing stage for selecting whether the human iris exists on the data set. The iris recognition was set up as the best, useful and adaptable security activity. therefore, the identification of a person should be fast and with a high precision rate. in this paper, an improvement framework was established and carried out. the aim of this paper is to design and create another method for more accurate iris discrimination. As shown in Table 3, the information collections of CASIA have achieved exceptional results. The information collection of the CASIA dataset has achieved a recognition rate of 99.7%. It can be observed that in iris recognition, the critical phase is the division. This is because biometric formats are spoiled when recognition is incorrectly performed on regions in the iris image as iris districts, resulting in helpless recognition.

ACKNOWLEDGEMENT

We extend our profound gratitude to the ICESCO Research Chair for AI Ethics for their unwavering support and valuable insights throughout the development and evaluation of the File Encryption by Iris Recognition System. Their dedication to fostering innovation in ethical artificial intelligence has been invaluable to the success of this project.

DECLARATION OF COMPETING INTEREST

None.

REFERENCES

Adamović, S., Miškovic, V., Maček, N., Milosavljević, M., Šarac, M., Saračević, M., & Gnjatović, M. 2020. An efficient novel approach for iris recognition based on stylometric FEATURESand machine learning techniques. *Future Generation Computer Systems* 107: 144-157.

Ahmadi, N., Nilashi, M., Samad, S., Rashid, T. A., & Ahmadi, H. 2019. An intelligent method for IRIS RECOGNITION using supervised machine learning techniques. *Optics & Laser Technology* 120: 105701.

Barpanda, S. S., Majhi, B., Sa, P. K., Sangaiah, A. K., & Bakshi, S. 2019. Iris feature extraction through wavelet mel-frequency cepstrum coefficients. *Optics & Laser Technology* 110: 13-23.

Chen, C. L., & Wu, C. C. 2020. Pupils' behavioral intention to use and achievements in ICT-Integrated mathematics remedial instruction: Case study of a calculus course. *Computers & Education* 145: 103740.

Chinese Academy of Sciences –"Institute of Automation Iris Database. http://www.cbsr.ia.ac.cn/english/Databases.asp.

Drozdowski, P., Rathgeb, C., & Busch, C. 2019. Computational workload in biometric identification systems: an overview. *IET Biometrics* 8(6): 351-368.

Dutta, S., Pandey, N., & Khatri, S. K. 2018. Microcontroller Based Bank Locker security System Using iris Scanner and Vein Scanner. In 2018 International Conference on Inventive Research in Computing Applications (ICIRCA) (pp. 53-57). IEEE.

Grünenberg, K., Møhl, P., Olwig, K. F., & Simonsen, A. 2020. Issue Introduction: IDentities and Identity: Biometric Technologies, Borders and Migration. Ethnos, 1-12.

Gu, J., & Jung, J. H. 2021. Adaptive Gaussian radial basis function methods for initial value problems: Construction and comparison with adaptive multiquadric radial basis function methods. *Journal of Computational and Applied Mathematics* 381: 113036.

Gumaei, A., Sammouda, R., Al-Salman, A. M. S., & Alsanad, A. 2019. Anti-spoofing cloud-based multi-spectral biometric identification system for enterprise security and privacy-preservation. *Journal of Parallel and Distributed Computing* 124: 27-40.

Guo, H., Li, B., Zhang, Y., Zhang, Y., Li, W., Qiao, F., & Zhou, S. 2020. Gait recognition Based on the Feature Extraction of Gabor filter and Linear Discriminant Analysis and Improved Local Coupled Extreme Learning Machine. Mathematical Problems in Engineering, 2020.

H. Geiger, "Facial recognition and Privacy". Center for Democracy & Technology. Available: https://cdt.org/blog/facial-recognition-and-privacy/

Hofbauer, H., Jalilian, E., & Uhl, A. 2019. Exploiting superior CNN-based iris segmentation for better recognition accuracy. *Pattern Recognition Letters* 120: 17-23.

Li, S., Song, W., Fang, L., Chen, Y., Ghamisi, P., & Benediktsson, J. A. 2019. Deep learning for hyperspectral image classification: An overview. *IEEE Transactions on Geoscience and Remote Sensing* 57(9): 6690-6709.

Murdock, W. Q., & Williams, P. A. 2017. U.S. Patent No. 9,662,558. Washington, DC: U.S. Patent and Trademark Office.

Muthukumar, A., & Kavipriya, A. 2019. A biometric system based on Gabor feature extraction with SVM classifier for Finger-Knuckle-Print. *Pattern RECOGNITION Letters* 125: 150-156.

Nguyen, K., Fookes, C., Jillela, R., Sridharan, S., & Ross, A. 2017. Long range iris recognition: A survey. *Pattern Recognition* 72: 123-143.

Ogbanufe, O., & Kim, D. J. 2018. Comparing fingerprint-based biometrics authentication versus traditional authentication methods for e-payment. *Decision Support Systems* 106: 1-14.

Perna, S. N., Margicin, J. M., Clifton, M. A., Jongjin, K. I. M., Varma, B. S., Piro, S. J., ... & Green, J. T. 2017. U.S. Patent No. 9,836,648. Washington, DC: U.S. Patent and Trademark Office.

Rivetti, C., Allen, T. E., Brown, J. B., Butler, E., Carmichael, P. L., Colbourne, J. K., ... & Campos, B. 2020. Vision of a near future: Bridging the human health–environment divide. Toward an integrated strategy to understand mechanisms across species for chemical safety assessment. *Toxicology in Vitro* 62: 104692.

Sahmoud, S., & Fathee, H. N. 2020, February. Fast iris segmentation algorithm for visible wavelength images based on multi-color space. In *International Conference on Advanced Concepts for Intelligent Vision Systems* (pp. 239-250). Springer, Cham.

Selvamuthukumaran, S., Ramkumar, T., & Shantharajah, S. 2020. An optimized rubber sheet model for normalization phase of iris recognition. *Computer Science and Information Technologies* 1(3): 126-134.

Sinha, V. K., Gupta, A. K., & Mahajan, M. 2018. Detecting fake iris in iris bio-metric system. *Digital Investigation* 25: 97-104.

Soliman, R. F., Amin, M., & Abd El-Samie, F. E. 2020. Cancelable iris recognition system based on comb FILTER. *Multimedia Tools and Applications* 79(3): 2521-2541.

Spettel, K., Barousch, W., Makristathis, A., Zeller, I., Nehr, M., Selitsch, B., ... & Willinger, B. 2019. Analysis of antifungal resistance genes in Candida albicans and Candida glabrata using next generation sequencing. *PloS One* 14(1): e0210397.

Sujatha, E., & Chilambuchelvan, A. 2018. Multimodal biometric authentication algorithm using iris, palm print, face and signature with encoded dwt. *Wireless PERSON al Communications* 99(1): 23-34.

Trokielewicz, M., Czajka, A., & Maciejewicz, P. 2020. Post-mortem iris recognition with deep-learning-based image segmentation. *Image and Vision Computing* 94: 103866.

Wang, Y., & Shan, S. 2021. Accurate disease detection quantification of iris based retinal images using random implication image classifier technique. *Microprocessors and Microsystems* 80: 103350.